

Electronic Supporting Information
for
Polyphenol derived bioactive carbon quantum dots incorporated
multifunctional hydrogel as oxidative stress attenuator for antiaging and *in*
***vivo* wound-healing applications**

Md Moniruzzaman^{1†}, Sayan Deb Dutta^{2†}, Jin Hexiu^{3†}, Keya Ganguly², Ki-Taek Lim^{2*}, and
Jongsung Kim^{1*}

¹Department of Chemical and Biological Engineering, Gachon University, 1342 Seongnam-daero, Seongnam-si, Gyeonggi-do 13120, Republic of Korea

²Department of Biosystems Engineering, Kangwon National University, Chuncheon-24341, Gangwon-do, Republic of Korea.

³Department of Plastic and Traumatic Surgery, Capital Medical University, Beijing-100069, Fengtai, China.

†These authors contributed equally to this manuscript.

*Corresponding authors: ktlim@kangwon.ac.kr (K.T. Lim) and jongkim@gachon.ac.kr (J. Kim)

Table of Contents

S. No.	Contents	Fig. No.
1.	Chemicals and instrumentation	
2.	Experimental section	
	2.1. CQDs synthesis	
	2.2. <i>In vitro</i> antioxidant properties	
	2.3. <i>In vitro</i> anti-aging properties	
	2.3.1. Collagenase inhibition assay	
	2.3.2. Tyrosinase and elastase inhibition assay	
	2.4. Synthesis and fabrication of GelMA-CQDs hydrogels	
	2.5. Characterization of GelMA-CQD hydrogel	
	2.6. <i>In vitro</i> cytotoxicity evaluation of GelMA-CQD hydrogels	
	2.7. <i>In vivo</i> wound healing efficacy of GelMA-CQD hydrogels	
3.	Digital images of 1,3,5-trihydroxybenzene, G-CQDs, and Y-CQDs.....	S1
4.	¹ H-NMR and ¹³ C-NMR spectra of 1,3,5-trihydroxybenzene, G- and Y-CQDs.....	S2
5.	XRD patterns and Raman spectra of 1,3,5-trihydroxybenzene, G- and Y-CQDs.....	S3
6.	Antioxidant effects of G-, and Y-CQDs in the cellular levels.....	S4
7.	Digital photographs of the GelMA–CQD hydrogels under visible and UV light	S5
8.	FT-IR spectra of the pure GelMA, GelMA–G, and GelMA–Y hydrogels.....	S6
9.	Cell migration quantification in the presence of scaffold leaching media	S7

1. Chemicals and instrumentation

1,3,5-trihydroxybenzene, i.e., ($C_7H_6O_4$); sulfuric acid (H_2SO_4); All chemical reagents were used without further purification. Deionized (DI) water was used throughout experiments and the synthesis process. PL spectrometer (Quanta Master, Photon Technology International, NJ, USA) instrument was used to record PL spectra. UV–Vis spectrophotometer (Varian Cary 100) instrument was used to measure ultraviolet–visible (UV–vis) absorption spectra. Microscope (JEM 3010, JEOL Ltd., Japan) instrument measured High-resolution transmission electron microscopy (HR-TEM) images of the as-prepared B-, G-, and Y- CQDs. FT-IR spectrometer (Bruker Vertex 70) measured Fourier transform infrared (FT-IR) spectra. X-ray photoelectron spectroscopy (XPS) was performed using an X-ray source with a twin-anode ($Al-K\alpha$, $h\nu = 1486.6$ eV) gun and a monochromatic gun. X-ray diffraction (XRD) spectra were collected using a Smart-Lab instrument (Rigaku) with a 4-kW X-ray generator and a D/teX Ultra 250 detector. Raman spectra were recorded via micro-Raman spectroscopy (ANDOR Monora500i, 633 nm).

2. Experimental section

2.1 Synthesis of dual-emissive CQDs

For a typical synthesis procedure, 1,3,5-trihydroxybenzene (200 mg) was added to a 100 mL glass beaker, followed by the addition of 2 mL of water and 2 mL of concentrated H_2SO_4 ¹⁷. The light yellowish solution was placed in a hot air oven preheated to 190 °C, and green and yellow CQDs (G-CQDs and Y-CQDs, respectively) were obtained after 50 and 90 min, respectively. After each reaction reached completion, the beaker was immediately removed from the oven and cooled naturally to room temperature. Next, 5 mL of deionized (DI) water was added to each beaker, the reaction mixtures were centrifuged at a high speed of 13000 rpm to collect the CQDs, which were then washed with water, followed by dialysis using a cellulose ester membrane with

a molecular weight cut-off of 500 Da for 72 h in DI water. The dialyzed products were dried and dispersed in ethanol, followed by filtration using a 0.22-micron filter for three filtration cycles. Lastly, the filtrates were dried to obtain black CQD powders (**Fig. S1, ESI†**).

2.2 *In vitro* antioxidant properties

The *in vitro* anti-oxidant property of the CQDs was evaluated using DPPH radical scavenging assay as reported previously [1]. Briefly, various concentration of CQDs (0 to 100 $\mu\text{g/mL}$) were mixed with 0.1 M DPPH-ethanol solution and incubated for 30 min at room temperature. After 30 min, the supernatant was collected and the absorbance was recorded at 516 nm. Ascorbic acid (0 to 100 $\mu\text{g/mL}$) were taken as positive control sets to compare the anti-oxidant property of CQDs. The radical scavenging efficiency was calculated using following equation:

$$\text{Scavenging efficiency (\%)} = (\text{Ab}_{\text{control}} - \text{Ab}_{\text{CQDs}}) / \text{Ab}_{\text{control}} \times 100$$

2.3 *In vitro* anti-aging properties

The *in vitro* anti-aging property was evaluated by means of aging-related enzyme inhibition study in the presence or absence of CQDs.

2.3.1. Collagenase inhibition assay

The collagenase inhibition assay was performed as reported in the previous literature [1]. Briefly, 4-phenylazobenzylloxocarbonyl-Pro-Leu-Gly-Pro-D-Arg trifluoroacetate was mixed with collagenase and dissolved in 1 mL of 0.1 M Tris-HCL buffer (pH 7.5). Next, CQDs with various concentrations (0 to 100 $\mu\text{g/mL}$) was mixed with 1.5 mg/mL of collagenase in the Eppendorf tube. After that, the mixture was incubated 30 min at room temperature and the reaction was stopped by adding 0.5 mL of 5% citric acid and 1 mL of ethyl acetate. After the reaction stopped,

the supernatant was collected and absorbance was recorded at 320 nm. The Collagenase inhibition activity was calculated using following equation:

$$\text{Collagenase inhibition activity (\%)} = (\text{Ab}_{\text{Control}} - \text{Ab}_{\text{CQDs}}) / \text{Ab}_{\text{Control}} \times 100$$

2.3.2. Tyrosinase and elastase inhibition assay

The tyrosinase inhibition activity was measured by a similar process as of collagenase assay by using 3,4-dihydroxy-L-phenylalanine (9.85 g dissolved in sodium phosphate buffer) and N-succinyl-Ala-Ala-Ala-p-nitroanilide (0.3 g dissolved in 1 mL of 0.5 M Tris-HCL, pH 8.6) as a substrate for tyrosinase and elastase. After that, the CQDs was added to the substrate containing tyrosinase and elastase enzymes and the reaction mixture was incubated for 30 min at room temperature. Next, the supernatant was collected from each experiment and the absorption was recorded at 475 nm (for tyrosinase) and 420 nm (for elastase), respectively. The enzyme inhibition activity was calculated using following equation:

$$\text{Enzyme inhibition activity (\%)} = (\text{Ab}_{\text{Control}} - \text{Ab}_{\text{CQDs}}) / \text{Ab}_{\text{Control}} \times 100$$

2.4 Synthesis of GelMA-CQD hydrogels

Methacrylated gelatin (GelMA) was synthesized as reported previously [2]. Briefly, 10g of Gelatin Type A was dissolved in PBS (pH 7.4), followed by addition of 2 mL of methacrylate anhydride under stirring at 40-45 °C for 2h. After 2h, the reaction was stopped by adding 2-fold warm PBS and stirred for 10 min. The solution was dialyzed against DI water using a dialysis tube (12-14 kDa cutoff molecular weight) for 5-7 days. Next, the GelMA solution was concentrated and lyophilized for 7 days to obtain a white foam. The GelMA-CQD scaffolds were fabricated by dissolving 10% GelMA in PBS with certain amount of CQDs (100 µg/mL) at 40-

45 °C. After that, 0.25% photoinitiator (LAP, Sigma-Aldrich, USA) was mixed the GelMA solution, and irradiated with 365 nm UV light (5 W) for 1 min. After UV exposure, the GelMA solution turned into semi-transparent hydrogel. Before cell culture and anti-microbial test, the hydrogels were washed with 1X PBS, and sterilized using UV light overnight. The GelMA-G-CQD and GelMA-Y-CQD containing hydrogels were designated as GelMA-G and GelMA-Y. Hydrogel devoid of CQDs were prepared as control sets.

2.5 Characterization of GelMA-CQD hydrogels

FE-SEM (SEM, Jeol, Japan) was used to investigate the morphology of the freeze-dried hydrogel scaffolds. The FT-IR spectrometer (Frontier, Perkin Elmer, UK) was used to evaluate the chemical interaction of developed scaffolds. The swelling and degradation property of the developed scaffolds were evaluated by immersing the scaffolds (GelMA, GelMA-G, and GelMA-Y) in PBS buffer as reported in our previous study [3, 4]. An ARES G2 rheometer (TA Instruments, USA) was used to measure the visco-elastic nature of the hydrogels using a 6 mm parallel plate at 37 °C. The GelMA hydrogels were characterized by flow and temperature sweep. The compressive strength and toughness of the developed hydrogels were evaluated using a uniaxial compressive loading through UTM (A&D digital, Japan). For compression measurement, a 1 × 1 cm hydrogel disc was used, respectively.

2.6 *In vitro* cytotoxicity evaluation of GelMA-CQD hydrogels

The *in vitro* anti-oxidative and anti-aging properties of the developed hydrogels were evaluated by DPPH radical scavenging assay and collagenase, tyrosinase, and elastase enzyme inhibition assay as mentioned in the section 1 and 2.

The cytotoxicity of the developed scaffolds was measured using WST-1 assay (DoGenBio, Republic of Korea) using human dermal fibroblast (hDFs) cells. Briefly, the hDFs (1.5×10^4 /well) were cultured in DMEM media in 96-well plate with sterilized hydrogels (GelMA, GelMA-G, and GelMA-Y) at 37 °C for 1, 3, and 5 days with 5% CO₂ environment. GelMA-treated cells were considered as control groups. After desired time point, the cells were incubated with 10 µL of WST-1 dye and the absorbance was recorded at 450 nm (625 nm as reference value) using a spectrophotometer (TECAN, Switzerland). All the experiments were triplicated ($n = 3$) and data are represented in mean OD \pm S.D. To access the viability, we have performed the live-dead assay (Sigma-Aldrich, USA) as per manufacturer's instruction.

Since, the viability of the hDFs were found higher in the presence of GelMA-Y hydrogels, therefore we investigated the cell morphology in the presence of GelMA-Y hydrogels against pure GelMA hydrogel. The morphology of the hDFs in the presence of GelMA-Y hydrogels were evaluated using immunocytochemistry (ICC) after 3 days of culture. Briefly, the hDFs were washed with PBS, fixed with 3.7% paraformaldehyde for 15 min, followed by permeabilization with Triton-X 100 for 50 min, and blocking with 1% bovine serum albumen for 1 h. After blocking, the cells were incubated primary and secondary antibody against vinculin (1:250 dilutions each) for 1 h, followed by incubation with 1-2 drops of Rhodamine-conjugated F-actin cytoskeleton probe (Thermo-Fischer Scientific, USA) for 30 min. After staining, the cells were mounted with anti-fade mounting media containing DAPI (Sigma-Aldrich, USA) and the cells were visualized using an inverted fluorescence microscope (Leica, Germany) with appropriate filters.

The *in vitro* wound healing property of the developed hydrogels were evaluated using scratch healing assay as described in our previous study [5]. Briefly, the hDFs were grown up to

80-90% confluency before wound healing study. After that, the cells were mechanically wounded using a 10 μ L sterile tip. The wounded layers were carefully washed with DMEM media to remove the cell debris, and incubated with hydrogel scaffold leaching DMEM media (prepared using 5 mg of each scaffolds incubated in DMEM media overnight at 37 °C) for 24 h. Cells without any scaffold's treatment was considered as control group. After 24 h, the wound area was photographed and the percentage of wound closure was calculated using ImageJ (v1.8, NIH, Bethesda, USA) software.

2.7 *In vivo* wound healing efficacy of GelMA-CQD hydrogels

The *in vivo* wound healing study was conducted to evaluate the wound healing property of the developed GelMA-CQD hydrogel scaffolds after 7 and 14 days of implantation in a subcutaneous wound model. For this, 3-4 weeks' old inbred control region (ICR) male rats (SPF Biotechnology, Beijing, China) were randomly divided into three groups: (1) Control group (GelMA only; $n = 3$), (2) GelMA-G group (Experimental group-1; $n = 3$), and (3) GelMA-Y (Experimental group-2; $n = 3$), respectively. The rats were supplied sufficient amount of food and water before experiments. Prior to surgery, the rats were anesthetized with 0.5% pentobarbital sodium (Sigma-Aldrich, USA). After that, the dorsal hairs were trimmed carefully and the skin was disinfected with 70% ethanol. Next, a circular 1 cm subcutaneous wound was generated using a biopsy punch. Next, 1 cm x 0.1 cm of hydrogel scaffold was carefully implanted into the wound area, and sealed with TagedremTM (Ningbo Finer Medical Instruments Co., China) adhesive wound dressing. Finally, the wound area was carefully sealed with a sterile gauze and placed in a sound-proof humidified chamber. The rats were monitored daily to check any adverse effects of the surgery and supplied sufficient food and water.

After 7 and 14 days, the rats were evaluated to check the wound healing of the implanted region. The dorsal surgical site was carefully photographed without harming the rats. After 14 days, the rats from all the groups were sacrificed and the wounded area was subjected to H&E staining to investigate the healing percentage. To evaluate the skin re-epithelialization and collagen deposition Masson's trichrome staining was performed.

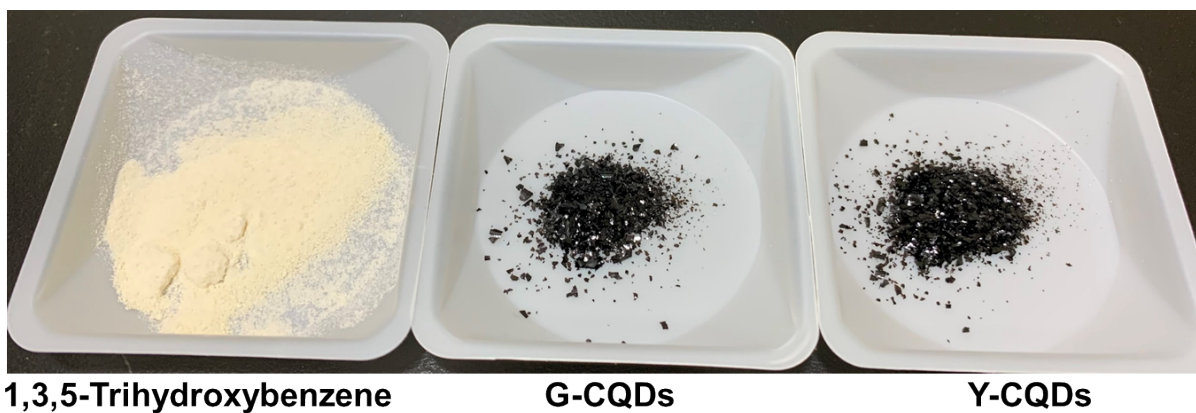


Fig. S1. Digital photographic images of 1,3,5-trihydroxybenzene, G-CQDs, and Y-CQDs powder.

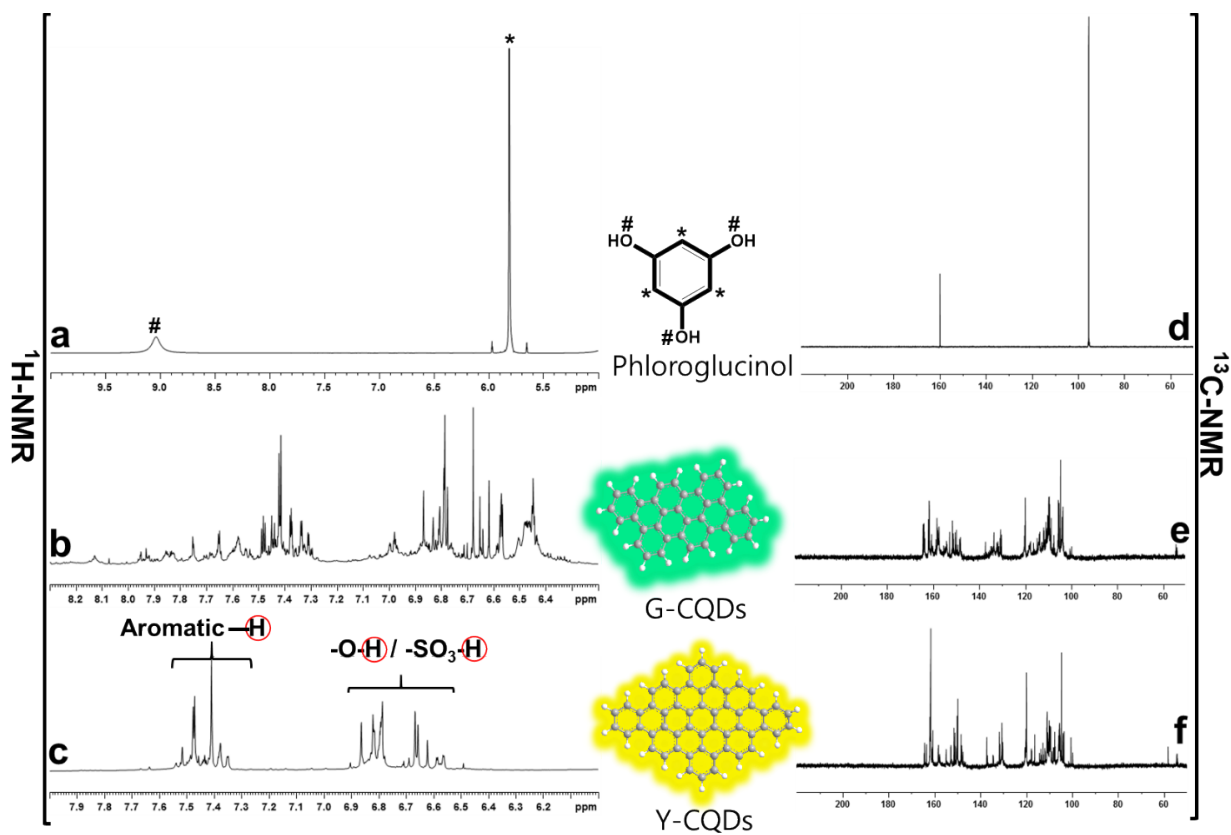


Fig. S2. (a)–(c) ^1H -NMR and (d)–(f) ^{13}C -NMR spectra of 1,3,5-trihydroxybenzene and the G and Y-CQDs.

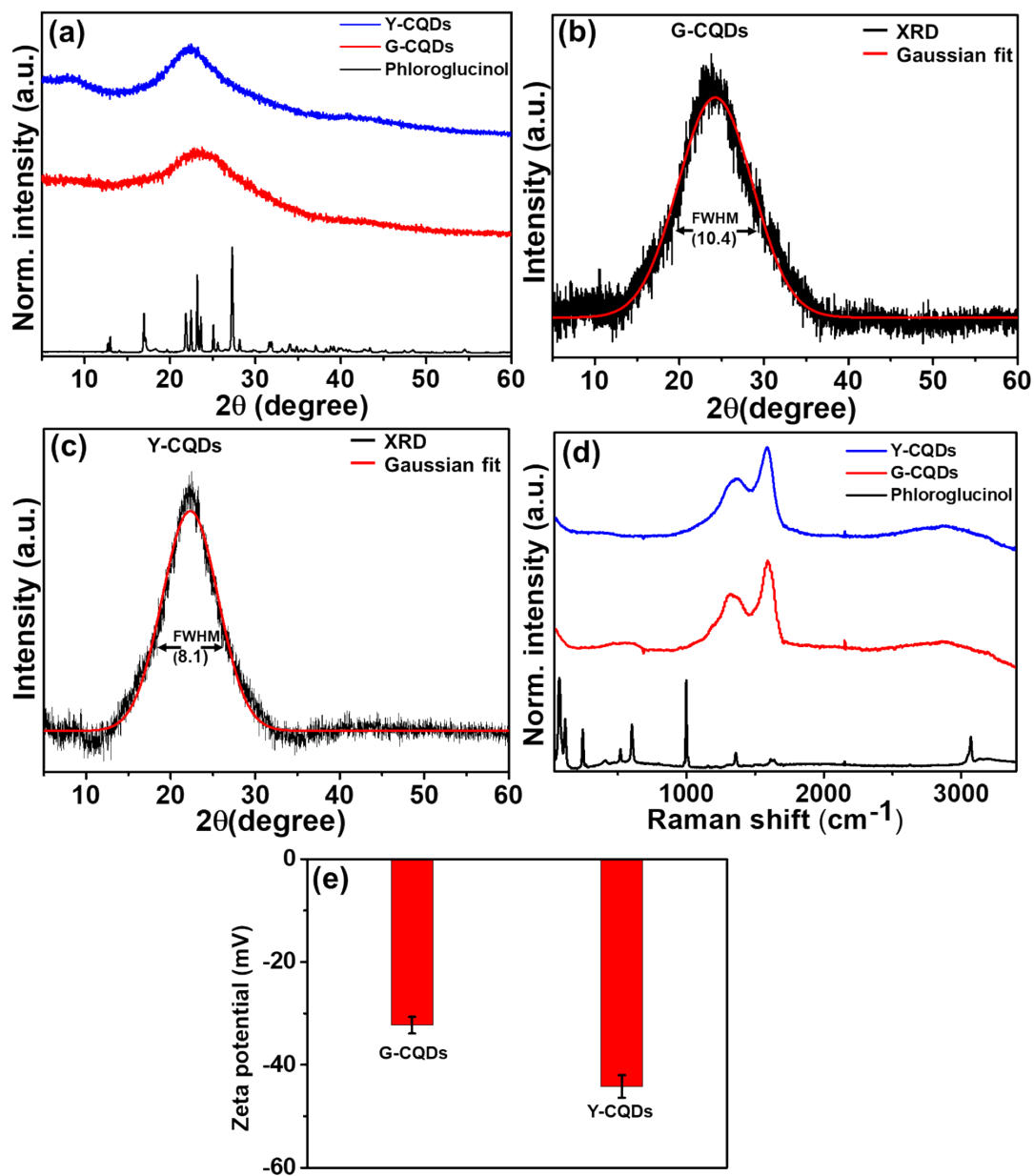


Fig. S3. (a) XRD patterns; (b & c) Gaussian fitted XRD spectra with FWHM value; (d) Raman spectra of 1,3,5-trihydroxybenzene and the G- and Y-CQDs; and (e) Zeta potential value of G-, and Y-CQDs.

Table S1: Average size of the crystallite or particle derived using Scherrer equation.

Sample	Peak position (2θ)	FWHM (2θ)	Crystallite size (or particle size)
G-CQDs	23.4	10.37	7.8
Y-CQDs	22.4	8.1	10

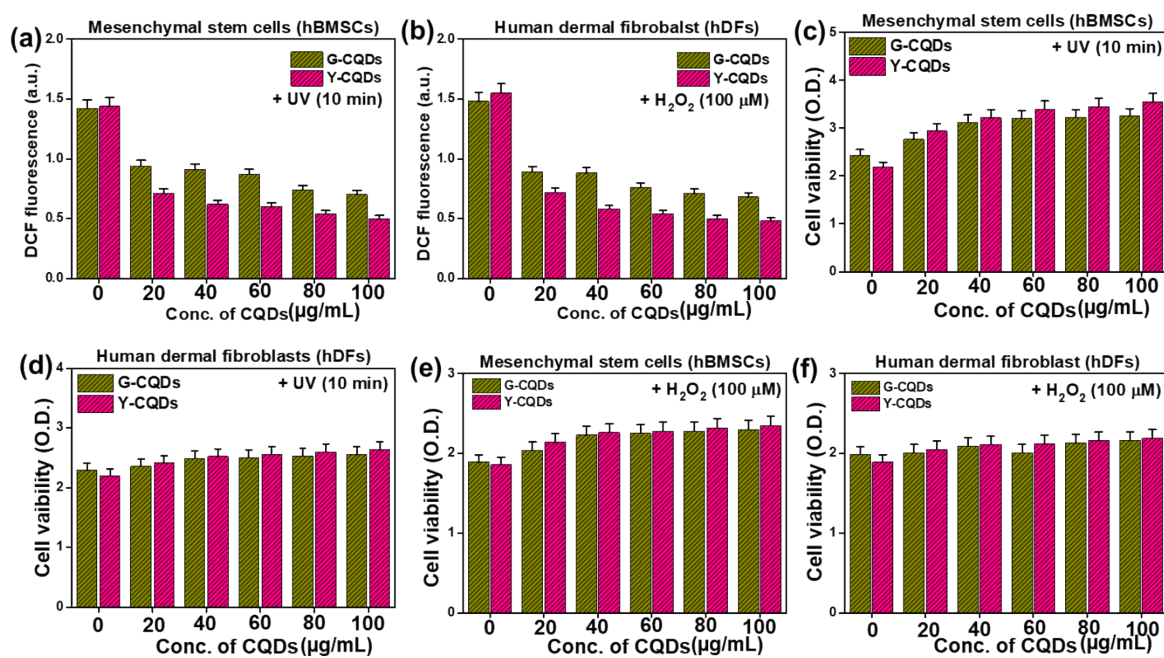


Fig. S4. Antioxidant effects of G- and Y-CQDs in the hBMSCs and hDFs cells (a & b). Inhibitory effects of G, and Y-CQDs against the UV (c & d) and H₂O₂ (e & f) induced ROS generation in hBMSCs and hDFs cells.

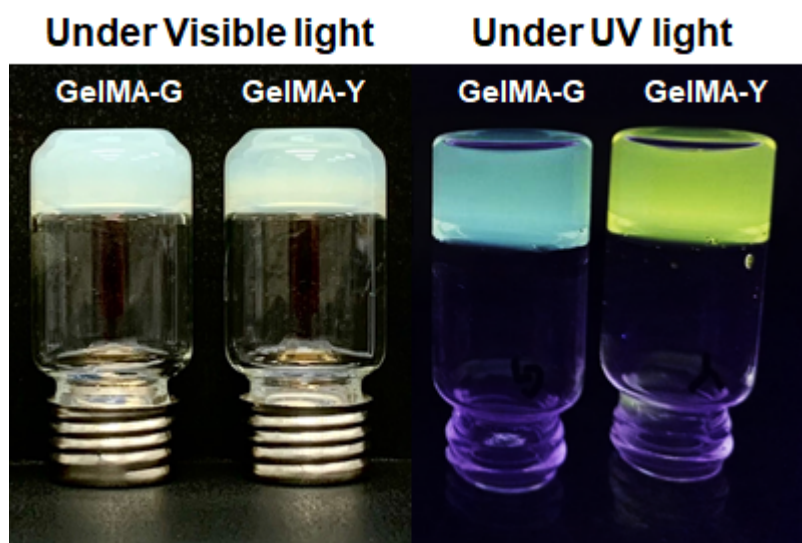


Fig. S5. Digital photographs of the GelMA–CQD hydrogels under visible light (left) and 365 nm UV light (right) irradiation illustrating the bright green and yellow colors of the GelMA–G and GelMA–Y hydrogels, respectively.

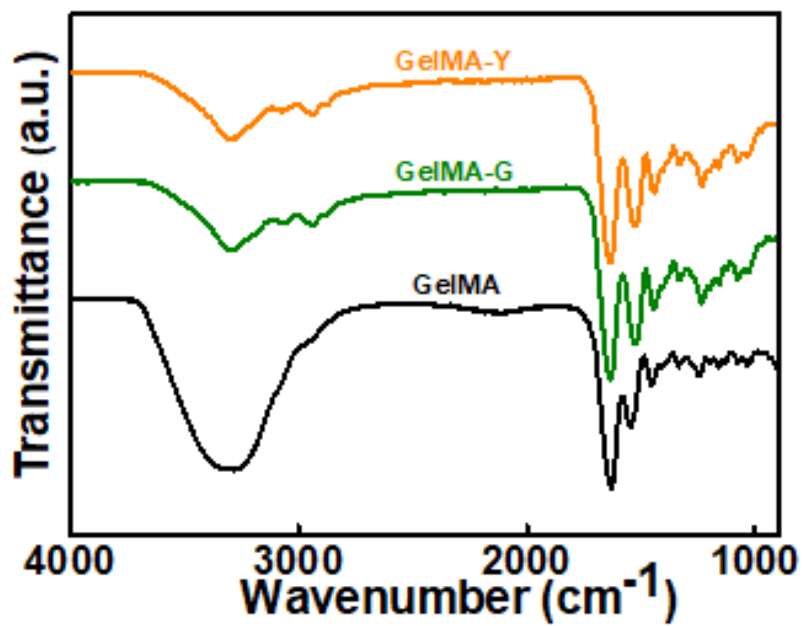


Fig. S6. FT-IR spectra of the pure GelMA, GelMA-G, and GelMA-Y hydrogels.

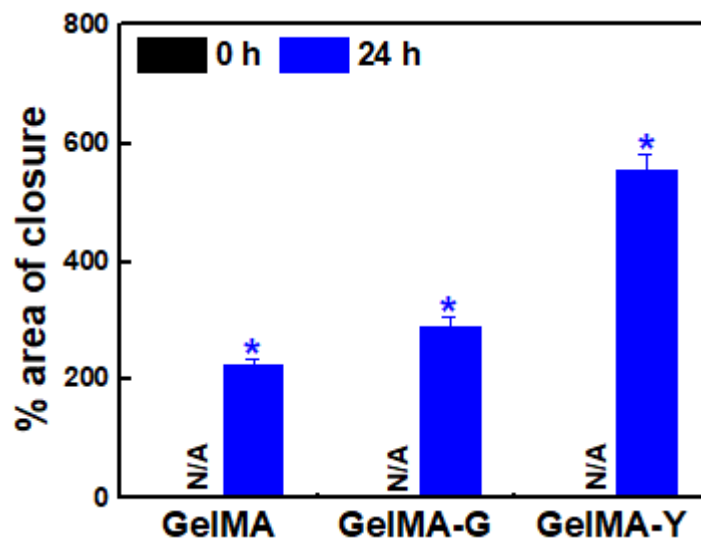


Fig. S7. Cell migration quantification in the presence of scaffold leaching media. Data are reported as means \pm SDs of triplicate experiments; statistical significance at $*p < 0.05$.

References:

- [1] Son MH, Park SW, Jung YK. Antioxidant and anti-aging carbon quantum dots using tannic acid. *Nanotechnology*. 2021;32:415102.
- [2] Geng B, Fang F, Li P, Xu S, Pan D, Zhang Y, et al. Surface charge-dependent osteogenic behaviors of edge-functionalized graphene quantum dots. *Chemical Engineering Journal*. 2021;417:128125.
- [3] Dutta SD, Hexiu J, Patel DK, Ganguly K, Lim K-T. 3D-printed bioactive and biodegradable hydrogel scaffolds of alginate/gelatin/cellulose nanocrystals for tissue engineering. *International Journal of Biological Macromolecules*. 2021;167:644-58.
- [4] Patel DK, Dutta SD, Hexiu J, Ganguly K, Lim K-T. 3D-printable chitosan/silk fibroin/cellulose nanoparticle scaffolds for bone regeneration via M2 macrophage polarization. *Carbohydrate Polymers*. 2022:119077.
- [5] Dutta SD, Park T, Ganguly K, Patel DK, Bin J, Kim M-C, et al. Evaluation of the Sensing Potential of Stem Cell-Secreted Proteins via a Microchip Device under Electromagnetic Field Stimulation. *ACS Applied Bio Materials*. 2021;4:6853-64.